Preprint of paper published as Nucl. Instr. Meth. Phys. Res. B 244 (2006) 377.

Molecular dynamics simulations of helium cluster formation in tungsten

K. O. E. Henriksson,* K. Nordlund, and J. Keinonen
Accelerator Laboratory, P. O. Box 43, FIN-00014 University of Helsinki, Finland
(Dated: April 12, 2005)

Molecular dynamics simulations of helium implantation into single-crystalline tungsten at 0 and 300 K have been performed. Non-damaging ion energies of 50, 100 and 200 eV were used. Clusters containing up to the order of 100 He atoms were formed. These clusters were nucleated athermally, via the creation of (111) crowdion interstitials and interstitial dislocation loop punching. Ruptures of He clusters were observed, but no associated ejection of W atoms.

PACS numbers: 61.72.Qq, 61.72.Ww, 83.10.Mj

I. INTRODUCTION

In this study we examine the formation and growth of helium clusters inside perfect tungsten, subjected to high-flux non-damaging irradiation. Before presenting the motivation for this study, we give a brief review of what has previously been done on the topic of He clusters (or, equivalently, clusters) in solids.

A. Formation and growth of helium clusters

Trapping of gas ions in solids was first observed in 1858 in direct-current gas discharge experiments carried out by Plücker, who found that the color of the discharge changed over time[1]. Plücker discovered that this phenomenon was caused by loss of gas into the electrodes. Subsequent experiments in this field showed that the results which were easiest to reproduce were those obtained by implantation of noble gases.

Turning to the specific noble gas He, it may be noted that Barnes *et al.* [2] were among the first researchers to observe cluster formation in metals (Cu, Al, and Be) irradiated with He. They discovered that clusters grew only in samples that had been annealed. The growth was attributed to thermal vacancies. This conclusion was challenged in 1973 when Sass and Eyre[3] found evidence for growth of He clusters in Mo at room temperature, where the contribution from thermal vacancies should be insignificant. Similar findings were obtained by Mazey *et al.* [4] in 1977.

A solution to the 'growth mechanism' problem was proposed in 1978 by Caspers *et al.* [5], who investigated He in Mo. The solution was called 'trap mutation', which was proposed to work as follows. Assuming the He atoms which form the cluster are all contained in a single vacancy, the addition of one extra He atom will cause the vacancy to mutate into a divacancy, resulting in expulsion of a self-interstitial atom (SIA) into the surrounding lattice. If there are n He atoms in the cluster, the trap mutation 'reaction' can be written $\mathrm{He} + \mathrm{He}_n\mathrm{V} \rightarrow \mathrm{He}_{n+1}\mathrm{V}_2 + \mathrm{I}$, where V denotes a vacancy and I a SIA. Trap mutation has been observed by at least Abd El Keriem *et al.* [6] for He in W. According to Abd El Keriem *et al.* the mutation in W takes place when 10 or more He atoms have been trapped by a single vacancy.

The fate of the expelled SIA and the effect on the surrounding medium has been elucidated by *e.g.* Evans, van Veen and Caspers[7] studying 150 eV He implantation at room temperature into single-crystalline, predamaged and annealed (001) Mo. Helium platelets were observed, and it was found that these grew by punching out interstitial loops in the (111) direction (a pressure-releaving mechanism originally proposed by Greenwod *et al.* (see Ref. 7 and references therein)). A density of 2-3 He/V was estimated.

In this context it may be of interest to review the possible trapping sites for He in metals. In the above discussion it was mentioned that vacancies can trap He atoms. This was observed by Kornelsen and Edwards in 1972 and 1974 (Ref. 8 and those in Ref. 1) and van Veen and Caspers in 1979 (Ref. in 1), who investigated He in W, Mo, and Ni. The vacancies may be native or created during the irradiation.

Kornelsen[8] also found that inert gas atoms such as He and Kr associated with vacancies are able to trap He atoms (in (001) W), verifying that He atoms should be able to form clusters. Interstitial C and O atoms did not appear to act as traps. In addition, Kornelsen and van Gorkum[9] discovered that He-V (a He atom in a vacancy), Ne, Ar, Kr, and Xe atoms act as traps for He. For the inert gas impurities the binding energy of the cluster was observed to increase with the number of trapped He atoms (up to a number of 100 atoms), rendering these traps nucleation centers for clusters. This binding energy trend was opposite that for vacancies and helium-filled vacancies, for which the energy decreased with increasing trap occupancy. Finally, it was shown by van der Kolk *et al.* [10] that also the substitutional impurities Ag, Cu, Mn, Cr, Al and In are able to trap He atoms.

It should be noted that if defects and impurities are absent in the samples, and if non-damaging irradiation is used, it is not obvious from the above discussion that He clusters can not form.

Thomas, Swansiger and Baskes[11] have investigated ^{3}He introduced into the face-centered cubic (FCC) metal Ni via the so called tritium trick (tritium is implanted and decays to helium) in poly-crystalline and single-crystalline samples. They observed that despite the non-

damaging conditions He became trapped in the samples instead of diffusing out. Subsequent atomistic calculations by Wilson, Bisson and Baskes[12] showed that He atoms introduced into perfect Ni are able to form interstitial clusters, which act as traps for additional He atoms. When the interstitial cluster is large enough it is able to spontaneously create a Frenkel pair. For this particluar case of He in Ni, five clustered He atoms are able to create a vacancy-interstitial pair, and eight He atoms are able to create two vacancies and two interstitials. It should be noted that this growth mechanism is strictly speaking not the same as trap mutation, since the initial cluster is made up of interstitial atoms, not atoms caught in a vacancy.

Other experimental indications of spontaneous He cluster formation under non-damaging irradiation conditions have been provided by Thomas and Bastasz[13] who implanted 300 eV He ions at 100 K into annealed polycrystalline Au foils. Analysis of the defects indicated they consisted of He clusters with diameters of about 10 Å and self-interstitial clusters. In the absence of damage the formation of these defects were attributed to self-trapping of He atoms.

B. Aim of this work

The experimental and theoretical findings reported above indicate He atoms implanted into metals with the FCC lattice structure (such as Ni and Au) are able to form clusters also in the absence of radiation damage and native defects. In the present study we have chosen to investigate spontaneous cluster formation in the body centered cubic (BCC) metal tungsten (W). The selection of W as the matrix can be motivated as follows. The formation of clusters should be dependent on the 'softness' of the matrix. Since W is among the ten elastically hardest elements[14], having a bulk modulus which is close to twice that of gold's, it is a suitable material to study for the extent of spontaneous cluster nucleation.

Tungsten is of particular interest also since it has been included as a candidate material for the plasma-facing wall (the so called first wall) in the International Thermonuclear Experimental Reactor (ITER)[15–17]. Specifically, W is to be used in the divertor, which is the part designed to take the largest loads of heat and particles exiting the plasma. The irradiation conditions are such that $\sim 1-100$ eV deuterium (D) or tritium (T) ions with a peak flux of $\sim 10^{24}$ ions m^{-2} s^{-1} are incident on the divertor surface. The estimated He flux is $1-10\%$ of this, making it $\sim (0.1-1)\times 10^{23}$ ions m^{-2} s^{-1}.

If He atoms are able to cluster in defect-free W then they can grow under prolonged irradiation until they may form blisters, which are visible surface-near bubbles. If the pressure gets too large these blisters may rupture and erode material into the fusion plasma. The introduction of wall material into the plasma gives rise to energy losses, such that the higher the nuclear charge state (the Z value) of the material the greater the cooling effect[18]. Therefore the possible degrading effects of W are worse than for example of Be and C, which are also candidate materials for parts of the first wall and divertor, respectively[16].

Spontaneous cluster formation is possible also if the irradiation particles are H ions[19–21]. In the particular case of W, the clusters are formed at micrometer depths, several orders of magnitude larger than the projected range. In a related publication we propose an explanation for this[22], while we in the present study focus on He in W.

II. METHODS

A. Molecular Dynamics simulations

Molecular dynamics simulations (MDS) were used to implant 50, 100, and 200 eV He atoms into (001) W[47]. In this section we describe the details of the MDS pertinent to this study. A more extensive description of MDS (especially for the investigation of cascades) can be found elsewhere[23].

For the 50 eV, and the first series of 100 eV He implantations, the initial, pristine W sample consisted of $16\times 16\times 10$ unit cells, making the sides about 50.6 Å (x and y) and 31.7 Å (z) long. For the other implantation series larger crystallites with side lengths $L_x = L_y =$ 101.3 Å and $L_z = 50.6$ Å were used.

In order to model implantation into a bulk sample, the techniques of atom fixing and temperature scaling were used. Atoms in a 4 Å thick layer at the bottom of the sample were held fixed at their original positions at all times. Atoms in a 5 Å thick layer above this region had their velocities scaled towards zero using the Berendsen temperature control method[24]. This temperature control was also applied at the periodic x and y side walls, although no atoms were held fixed there. The simulation cell was periodic in x and y, but not in z.

The incident He atom in each of the runs is always started from the same horisontal position. In order to avoid an artifical buildup of He at the same location near the surface — which would not occur in a real experiment where the incident ions cover a large surface — the simulation cell was shifted at the start of each implantation run. This means that all atoms were moved by a random amount in the x direction, and then the positions were corrected using the periodicity. This was also done for the y direction.

Each successive implantation started with a He atom positioned outside the sample. The distance to any other atom was larger than the potential cutoff radius of 4.4 Å. Each incident He atom was directed towards the surface with a tilt (or polar) angle $\theta = 25°$ and a twist (or azimuthal) angle $\phi = 0$. We chose $\theta = 25°$ since range calculations showed the projected range to be minimal in this case. The initial energy of the He atom, 50, 100, or 200 eV, was well below the energy needed to create

damage in the W sample[25–27], which can be calculated as follows. The maximum kinetic energy transferred to a lattice atom by the projectile in a collision is given by $E' = 4m_1m_2/(m_1 + m_2)^2E$, where E is the energy of the incident atom and m_1, m_2 the masses of the lattice atom and the projectile, respectively[27]. For $^4_2$He ($m_1 = 4.0026$ u) and the average W atom ($m_2 = 183.84$ u) (see Ref. 28), and the maximum energy E' equal to the threshold energy of 42 ± 1 eV (in the (100) direction, see Ref. 29), the minimum He energy for damage production is $E = 503 \pm 12$ eV.

After starting the He recoil towards the surface, the evolution of the whole system is followed up to 5 ps. At the end of each implantation run the sample was quenched to zero Kelvin during the final 500 fs to avoid a continous heating-up of the sample from one implantation run to the next. At the start of the cooling the temperature was usually somewhere between 10 and 30 K.

The He flux to the smaller sample was 7.8×10^{27} ions m^{-2} s^{-1}, and for the larger sample 1.9×10^{27} ions m^{-2} s^{-1}.

For the W-W interaction an improved[30] Embedded-Atom Method (EAM) potential by Finnis and Sinclair was used. The He-He interaction was a pair-potential based on Density Functional Theory (DFT) calculations[31]. For the He-W interaction an *ab initio* based pair potential presented in an earlier study[32] was used.

B. Analysis of cluster nucleation

For each implantation run in all the 50, 100, and 200 eV He series the initial and final positions of atoms were compared. Atoms, whose initial and final positions differed by 1 Å or more were counted. If the total number of displaced host lattice atoms in a run exceeded some threshold value (mostly 4-5) the implantation run was resimulated and the displacements investigated in more detail.

For the selected runs the following elements of analysis were carried out: (a) For atoms displaced by 1 Å or more vectors were drawn from initial to final position. This made *e.g.* (111) crowdion interstitial events, where several host lattice atoms are coherently displaced in the (111) direction, easier to spot. (b) The motion of the displaced atoms was visually inspected. (c) The coordinate displacements Δx, Δy and Δz as well as the total displacement $\Delta r = \sqrt{(\Delta x)^2 + (\Delta y)^2 + (\Delta z)^2}$ were calculated. These were compared to the displacements of atoms in an ideal (111) crowdion interstitial. (d) If necessary, the atoms undergoing displacements were plotted as a function of time.

In W an atom in an ideal (111) crowdion interstitial is displaced by $\Delta r_0 = \frac{a}{2}\sqrt{3} = \Delta x_0\sqrt{3} = 2.74$ Å, where $a = 3.1652$ Å is the W BCC lattice parameter and $\Delta x_0 = 1.58$ is the ideal coordinate displacement along all three coordinate axes. When loking for crowdions, any W atom displacing such that $0.90 \leq \Delta x_i/\Delta x_{0,i} \leq 1.10, i = 1, 2, 3$ was labeled a crowdion. This gives the condition $2.44\text{Å} \leq \Delta r \leq 3.04\text{Å}$ for Δr.

When groups of adjacent crowdions were observed the displacement event was considered a loop punching event, *i.e.* the formation of an interstitial dislocation due to the high pressure in the cluster[33,34]. No further analysis, *e.g.* of the Burger's vector of the loops, was carried out.

C. Calculation of densitites and pressures

Densities of He clusters have been calculated in various cases. Here we outline the method used to obtain these values.

In order to calculate a density of a cluster, one has to first calculate the number of gas atoms in the cluster and then the volume these atoms occupy. The first calculation is straightforward. In general, the simplest way to calculate the volume of an atom (or vacancy) in the BCC lattice is to divide the volume of the conventional unit cell with the number of lattice atoms, *i.e.* 2, obtaining $V_v = a^3/2$. Such a method would not work for arbitrary systems of atoms, such as (liquid) He clusters. Therefore we have in this study adopted a volume definition which relies on the close-packing of atoms. With this method the volume of any atom is defined as $V_{a,cp} = 4\pi r^3/3$, where r is the shortest distance to any neighboring atom, divided by two. Here the label *cp* emphasizes that the close-packing volume definition is used.

Note that the volume of a vacancy in a perfect lattice is $V_{v,cp} = \sqrt{3}\pi a^3/16 \equiv r_{cp}a^3/2 = r_{cp}V_v$, where $r_{cp} = \sqrt{3}\pi/8 = 0.68$ is the close-packing ratio of the BCC lattice. With $a = 3.1652$ Å one obtains $V_v = 15.856$ Å^3 and $V_{v,cp} = 10.784$ Å^3 per vacancy.

From the atomic density ρ_{cp} or ρ (in units of atoms Å^{-3}) the number density n (in units of atoms per vacancy (V)) is calculated as $n = \rho_{cp}V_{v,cp} = (\rho/r_{cp})r_{cp}V_v = \rho V_v = 10.784 \times \rho_{cp}\text{Å}^3$ atoms/V $= 15.856 \times \rho\text{Å}^3$ atoms/V, *i.e.* n is independent of the method to calculate atomic volumes.

Whenever He cluster volumes V_b are mentioned the close-packing version is understood, since the computer codes that calculate the volumes use only the close-packing scheme.

Simulated pressures are compared to the Mills-Liebenberg-Bronson (MLB) semiempirical equation of state (EOS)[35]. This EOS is considered to be reasonably good[36] for ^{4}He up to pressures of 100 GPa, which is 50 times the original upper limit in the experiments from which the MLB EOS has been calculated. By 'reasonably good' it is meant that when the MLB prediction for the pressure is compared to theoretical calculations, the difference is not more than 50%. The original experimental limits were 75 K $< T <$ 300 K and 0.2 GPa $< P <$ 2 GPa, where T is the temperature and P the pressure[35].

D. Calculation of fluence-dependent properties

Various time-dependent properties of the clusters, *e.g.* pressure, have been calculated. When values for these properties are presented they are visually verified averages over short times $t_1 \leq t \leq t_2$, such that the value of the property in question has not experienced too violent changes which would make the average meaningless.

III. RESULTS

In the following results on the probability of backscattering and the flux test are presented first. After that the findings on nucleation and growth of clusters are presented and summarized. The last sections deal with cluster properties, the critical pressure for loop punching, and the possibility of superlattices.

A. Probability of backscattering

It may be of interest to have some estimates on the entrance probability of the impinging He atoms. In Table I we present values from TRIM calculations (TRIMC) and MDS for this probability. The probability is calculated as N_b/N_i, where N_b is the number of backscattered atoms and N_i the total number of impinging atoms. The TRIMC values are calculated using the SRIM-2003 software package[37], and an angle of incidence $\theta = 25°$ (off-normal). The W sample in the TRIMC was 1000 Å deep. Uncertainties in the counts were calculated using Poisson statistics.

TABLE I: TRIMC and MDS results for the probability of backscattering of He ions incident on W at an off-normal angle of 25°.

Ion energy	Backscattering probability	
(eV)	TRIMC	MDS
10	0.485 ± 0.008	
20	0.521 ± 0.009	1.00 ± 0.02
30	0.527 ± 0.009	
50	0.520 ± 0.009	0.764 ± 0.007
100	0.506 ± 0.009	0.654 ± 0.005
150	0.493 ± 0.009	
200	0.489 ± 0.009	0.592 ± 0.007
300	0.482 ± 0.008	
500	0.470 ± 0.008	
700	0.447 ± 0.008	
1000	0.442 ± 0.008	

B. Flux test

Kinetic Monte Carlo simulations (KMCS)[38,39] were carried out in order to find the minimum flux down to which our MDS results for the clustering depths remain similar. Run number 1000 of the 50 eV He implantation at 300 K was used to obtain the relevant parameters for the KMCS. This gives a fluence of 3.9×10^{19} He m^{-2} and an effective total migration time of 1000×4.5 ps $= 4.5$ ns (accounting for the 500 fs quenching time at the end of each run) since the start of the implantation series. The size of the target surface, the ion flux, the implantation profile (assumed Gaussian), and the average temperature of the implantation-heated target for this run were used as input parameters in the KMCS. The results of the flux test are presented in Table II, for a clustering radius of 3.16 Å. The radius is defined so that when the distance between two atoms or a cluster and an atom is smaller than this radius, then the two entities are considered to be clustered.

TABLE II: MDS and KMCS results for MDS run 1000 using different fluxes but the same fluence. The first group of data (the first line) contains the MDS result.

Flux (10^{17} He m^{-2} s^{-1})	Cluster depth (Å)
8.660×10^{10}	5.5 ± 0.4
8.660×10^{10}	6.55 ± 0.02
8.660×10^{9}	6.50 ± 0.01
8.660×10^{8}	6.56 ± 0.03
8.660×10^{7}	7.3 ± 0.2
8.660×10^{6}	11 ± 2
8.660×10^{5}	13 ± 2
8.660×10^{4}	26 ± 6
8.660×10^{3}	64 ± 15
8.660×10^{2}	149 ± 62
8.660×10^{1}	284 ± 90

C. Cluster nucleation and growth

Before presenting the numerical results it is useful to get an understanding of how the clusters grow in size or volume during the implantations. The initial cluster seeds consist of interstitial clusters, which form spontaneously in W when migrating He atoms come close enough to one another. The interstitial clusters are turned into substitutional clusters via ejection of W atoms in or close to tbe clusters, when they have reached a large enough number of contained He atoms.

The most common way for (substitutional) clusters to grow is by direct absorption of the hot He ion, which heats up the cluster and renders the contained gas atoms mobile inside their enclosure. This enables them to push on each other and collide with the atoms of the surrounding solid. If this motion is violent enough, W atoms will be pushed aside temporarily or permanently. Then the cluster may grow in volume and its pressure will be reduced. It is also possible for the cluster to leak He atoms if it is close enough to the surface.

Also, in the simulations it was noted that rupturing of

clusters does not start immediately when the He ion is caught in them. The overall picture is that the rupturing occurs relatively late, at around 1 ps or more since the implantation of the individual ions.

Results for runs 1-799 in the first 100 eV He implantation series have already been reported in Ref. 32. Those results will not be repeated here, but they will be included in the findings pertaining to all the relevant runs between 1 and 2585 (when the series was terminated due to a significant cluster rupture) in this implantation series.

In Table III an overview of the frequency of cluster growth events are given for the four 100 eV He implantation series investigated in detail. Here a cluster growth event is such an event where a cluster grows either in volume or occupancy (number of He atoms). Emptying of a cluster (atoms escaping from the cluster through the surface or into closeby clusters) is also considered a growth event, since a cavity capable of absorbing new He atoms, is formed.

The runs and fluences at which the first crowdion interstitial or loop-punching like events occurred are shown in Table IV, for the implantation series which have been investigated in detail. Only events where the clusters grow in occupancy have been considered. In Table V the temperatures and pressures in the clusters participating in the first loop punching like events are shown. 'Cluster 1' and 'Cluster 2' denotes the initial clusters which are fused, and 'Final cluster' denotes the cluster which is formed in conjunction with the loop-punching like event. Here NA means that the cluster actually was an atom, in most cases the incident He ion.

1. 100 eV, series 1

In about 15% of the 156 investigated runs the He ion either created (111) crowdion interstitials by itself or after it was caught in a small cluster of He atoms. About 13% of the runs displayed loop punching like events. In one run (corresponding to 0.6%) both crowdion and loop punching like events occurred. The other remaining runs, about 72%, did not reveal any other clearly discernible mechanism for cluster growth. However, in some of these runs we noticed what one could call internal crowdion like events, where W atoms are moving along lines connecting clusters to each other.

The first crowdion event where a He cluster grows occured in run 184, where a cluster containing two He atoms absorbed the incident He atom.

The first loop punching like event where a He cluster grew occured in run 402, where clusters containing 5 and 6 He atoms merged. At $0.3-0.5$ ps, before displacements: $\rho_{cp,1} = 0.392 \pm 0.002$ Å^{-3}, $\rho_{cp,2} = 0.426 \pm 0.007$ Å^{-3}. At $3.8-4.0$ ps, after displacements: $\rho_{cp} = 0.417 \pm 0.004$ Å^{-3}.

The detailed investigation of this series of implantation runs was ended after a cluster rupture event in run 2586. A cluster containing 236 He atoms was reduced to 64 He atoms. The average pressure and density values before rupture at about 0.7 ps were 37.6 ± 0.3 GPa and 0.321 ± 0.002 Å^{-3}, respectively. Shortly after stabilization, at about 16 ps, the values were 2.14 ± 0.05 GPa and 0.192 ± 0.001 Å^{-3}. Plots of pressure and number of atoms in the rupturing cluster are shown in Fig. 1.

In Table VI the pressure and atomic density of He clusters in some of the loop punching events are given. The runs not included in the list did not show any growth in the occupancy of the involved clusters. Some events in the table did exhibit both types of loop punching (volume and occupancy change) but the volume-growth type of these events (10 all in all) are not listed.

In Table VII we present a comparison between the measured atomic densities and that predicted by the MLB equation of state. The correspondence is not perfect, but at least the densities are remarkably good.

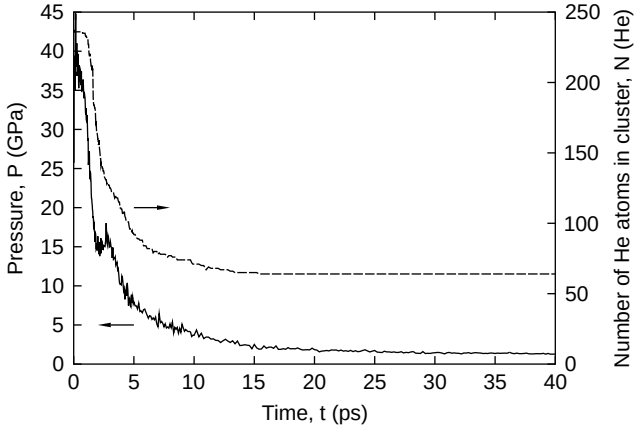

FIG. 1: Pressure and number of atoms in the shrinking cluster in run 2586 in the 100 eV He series 1.

2. 50 eV, series 1

In about 26% of the 85 investigated runs crowdion events were found. Loop punching like events were observed in 12% of the runs.

The first crowdion event where a He cluster grew occured in run 142, where a 'cluster' containing 2 He absorbed the He ion.

The first loop punching like event where a He cluster grew occured in run 715, where a cluster with 15 He grew by absorbing the He ion. At $0.0 - 0.2$ ps, before displacements: $\rho_{cp} = 0.43 \pm 0.01$ Å^{-3}. At $2.0 - 2.2$ ps, after displacements: $\rho_{cp} = 0.41 \pm 0.02$ Å^{-3}.

The detailed investigation of this series of implantation runs was ended after a cluster rupture event in run 2027. A cluster was reduced from 35 to 5 He atoms. The average temperature, pressure and density values before rupture, at about $0.6 - 0.8$ ps, were $T = 2010 \pm 40$ K,

TABLE III: Overview of cluster growth events for the implantation series investigated in detail. The number of runs that have been analyzed is N_i, and the number of runs where one or more (111) crowdion interstitials were observed is N_c. The quantity N_{lp} is similar to N_c but loop punching events were observed instead of crowdions. The run where a significant rupture of a surface-near cluster occurred is denoted N_{sr}.

Ion energy (eV)	Series	N_i	N_c			N_{lp}			N_{sr}
			$1-1000$	$1001-2000$	$2000-$	$1-1000$	$1001-2000$	$2000-$	
100	1, 0 K	156	21	2	0	5	8	7	2585
50	1, 0 K	85	16	7	0	5	5	0	2027
50	2, 0 K	70	14	11	0	3	4	0	1891
50	1, 300 K	113	12	12	4	3	4	6	2242

TABLE IV: Runs where the first crowdion and loop punching like events occurred in the implantation series investigated in detail. The events were such that He clusters grew in occupancy (number of contained He atoms).

Ion energy (eV)	Series	First crowdion event		First loop-punching event	
		Run number	Fluence (He m^{-2})	Run number	Fluence (He m^{-2})
100	1, 0 K	184	7.2×10^{18}	402	15.7×10^{18}
50	1, 0 K	142	5.5×10^{18}	715	27.9×10^{18}
50	2, 0 K	263	10.3×10^{18}	996	38.9×10^{18}
50	1, 300 K	138	5.4×10^{18}	453	17.7×10^{18}

TABLE V: Temperature and pressure changes for the clusters participating in the first loop punching like event for the implantation series investigated in detail. The events were such that He clusters grew in occupancy (number of contained He atoms). NA means that the cluster actually was an atom, in most cases the incident He ion.

Ion energy (eV)	Series	Cluster 1		Cluster 2		Final cluster	
		Temperature (K)	Pressure (GPa)	Temperature (K)	Pressure (GPa)	Temperature (K)	Pressure (GPa)
100	1, 0 K	3.5 ± 0.4	225 ± 1	1300 ± 100	227 ± 6	330 ± 20	187 ± 4
50	1, 0 K	6500 ± 600	203 ± 9	NA	NA	2600 ± 100	119 ± 6
50	2, 0 K	25 ± 4	185 ± 1	NA	NA	540 ± 80	76 ± 6
50	1, 300 K	3200 ± 1000	250 ± 20	NA	NA	646 ± 6	162 ± 7

TABLE VI: Growth type, pressure and density values for some loop punching-like events in runs in the 100 eV He series 1. The growth type '$m+n$' means that a cluster containing m He atoms has grown by absorbing n He atoms. These n atoms can be in another cluster, separate atoms, or a combination of these alternatives.

Run number	Growth	Pressure (GPa) changes		Atomic density ρ_{cp} (He/Å^3) changes	
		Before	After	Before	After
402	6+5	227 ± 6	187 ± 4	0.426 ± 0.007	0.417 ± 0.004
720	22+0	111.96 ± 0.04	93 ± 1	0.3596 ± 0.0001	0.343 ± 0.001
1035	4+0	244 ± 1	216 ± 7	0.455 ± 0.010	0.4552 ± 0.0010
	5+0	194 ± 1	187 ± 1	0.4069 ± 0.0009	0.422 ± 0.006
1037	24+0	78.8 ± 0.3	65.8 ± 0.6	0.3312 ± 0.0003	0.328 ± 0.003
	26+8	169 ± 3	84 ± 3	0.457 ± 0.007	0.387 ± 0.006
1450	13+0	108.30 ± 0.04	96.9 ± 0.6	0.36204 ± 0.00003	0.351 ± 0.001
1451	15+0	111.4 ± 0.4	98 ± 1	0.3709 ± 0.0005	0.352 ± 0.002
1452	13+0	122.6 ± 0.9	101.2 ± 1.1	0.370 ± 0.001	0.354 ± 0.003
	30+0	92.5 ± 0.2	93.0 ± 0.3	0.3471 ± 0.0006	0.350 ± 0.002
1478	6+2	249 ± 12	150 ± 10	0.43 ± 0.01	0.38 ± 0.02
1869	11+7[a]	169.2 ± 0.2	124 ± 1	0.4025 ± 0.0001	0.377 ± 0.002
	73+18	77.1 ± 0.3	68.9 ± 0.5	0.3449 ± 0.0007	0.346 ± 0.002
1926	111+3	50.42 ± 0.11	48.1 ± 0.6	0.3153 ± 0.0004	0.3299 ± 0.0011
2070	5+2	185 ± 1	145 ± 5	0.4294 ± 0.0004	0.406 ± 0.012
2087	129+0	38.57 ± 0.04	36.02 ± 0.02	0.28999 ± 0.00010	0.2858 ± 0.0001
2088	129+0	45.3 ± 0.2	36.6 ± 0.3	0.3329 ± 0.0007	0.3113 ± 0.0008
2370	184+5	47.7 ± 0.4	38.1 ± 0.6	0.353 ± 0.002	0.333 ± 0.002
2581	226+2	34.41 ± 0.08	32.36 ± 0.09	0.3003 ± 0.0003	0.3019 ± 0.0007

[a]The 18-atom cluster formed here is fused with the 73-atom cluster on the following line.

TABLE VII: Atomic density of clusters after loop punching like event has occured in runs in the 100 eV He series 1.

Run	Growth	Atomic densities ρ_{cp} (He/Å^3)	
		Simulated	MLB
402	6+5	0.417 ± 0.004	0.477
720	22+0	0.343 ± 0.001	0.436
1035	4+0	0.4552 ± 0.0010	0.552
	5+0	0.422 ± 0.006	0.525
1037	24+0	0.328 ± 0.003	0.367
	26+8	0.387 ± 0.006	0.304
1450	13+0	0.351 ± 0.001	0.458
1451	15+0	0.352 ± 0.002	0.435
1452	13+0	0.354 ± 0.003	0.429
	30+0	0.350 ± 0.002	0.423
1478	6+2	0.38 ± 0.02	0.349
1869	11+7	0.377 ± 0.002	0.374
	73+18	0.346 ± 0.002	0.362
1926	111+3	0.3299 ± 0.0011	0.314
2070	5+2	0.406 ± 0.012	0.353
2087	129+0	0.2858 ± 0.0001	0.368
2088	129+0	0.3113 ± 0.0008	0.291
2370	184+5	0.333 ± 0.002	0.276
2581	226+2	0.3019 ± 0.0007	0.286

$P = 102 \pm 2$ GPa and $\rho_{cp} = 0.418 \pm 0.006$ Å^{-3}. After rupture, there were 5 He atoms in the cluster. At $3.4 - 3.6$ ps: $T = 490 \pm 80$ K, $P = 22 \pm 3$ GPa and $\rho_{cp} = 0.26 \pm 0.02$ Å^{-3}. Plots of pressure and number of atoms in the rupturing cluster are shown in Fig. 2.

In Fig. 3 the evolution of the irradiated target is shown for run 2027.

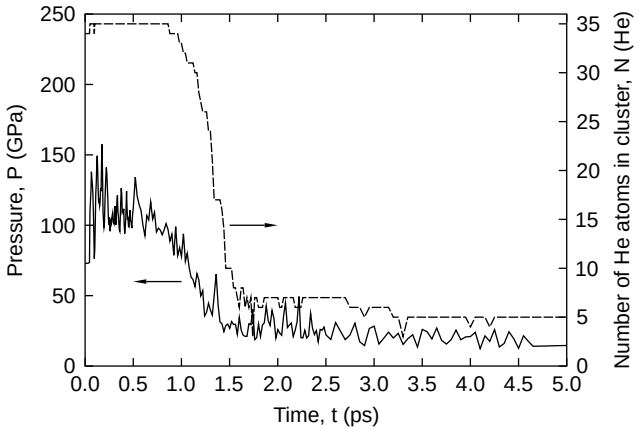

FIG. 2: Pressure and number of atoms in the shrinking cluster in run 2027 in the 50 eV He series 1.

3. 50 eV, series 2

In about 34% of the 70 investigated runs crowdion events were found. Loop punching like events were observed in 10% of the runs. In one run (corresponding to 1%) both crowdion and loop punching like events occurred.

The first crowdion event where a He cluster grew occured in run 263, where a He passing a loosely bound He dimer was caught by a nearby He atom. The motion of the formed He dimer activated the loosely bound dimer, and both fused into a 4 He cluster. A crowdion with 5 W was formed.

The first loop punching like event where a He cluster grew occured in run 996, where a cluster with 8 He grew by absorbing the He ion. Two (111) rows, containing 3+4 W, were punched out. The cluster was near the surface, below a surface vacancy, and some of the clustered atoms were able to escape from the sample. The cluster was reduced to 3 He atoms at about 2 ps. At $0-0.2$ ps: $\rho_{cp} = 0.419 \pm 0.001$ Å^{-3}. At $2 - 2.2$ ps: $\rho_{cp} = 0.34 \pm 0.02$ Å^{-3}.

The detailed investigation of this series of implantation runs was ended after a cluster rupture event in run 1891. A cluster containing 25 He atoms was evaporated after a collision with the He ion. The average temperature, pressure and density values before rupture at about $0 - 0.1$ ps were $T = 3500 \pm 800$ K, $P = 99 \pm 8$ GPa and $\rho_{cp} = 0.355 \pm 0.008$ Å^{-3}.

4. 50 eV, series 1, 300 K

In about 25% of the 113 investigated runs crowdion events were found. Loop punching like events were observed in 12% of the runs. In five runs (corresponding to 4%) both crowdion and loop punching like events occurred.

The first crowdion event where a He cluster grew occured in run 138, where the He ion joined an isolated He atom and formed a dimer, causing the formation of a crowdion interstitial displacing 2 W atoms.

The first loop punching like event where a He cluster grew occured in run 453, where a cluster with 9 He grew by absorbing the He ion at 0.1 ps after implantation. The loop punching event involved 3 rows, containing $3+5+3$ W atoms. At $0 - 0.1$ ps: $\rho_{cp} = 0.439 \pm 0.008$ Å^{-3}. At $4.3 - 4.5$ ps: $\rho_{cp} = 0.43 \pm 0.02$ Å^{-3}.

The detailed investigation of this series of implantation runs was ended after a cluster rupture event in run 2242. A cluster containing 27 He atoms catched the He ion, but was unable to keep the cluster together. Consequently, 23 W atoms in 5 rows of approximately equal length were displaced towards the surface, while He atoms escaped from the cluster through the surface. The average temperature, pressure and density values just before rupture at about $2.9 - 3.1$ ps were $T = 1300 \pm 110$ K, $P = 101 \pm 6$ GPa and $\rho_{cp} = 0.41 \pm 0.01$ Å^{-3}.

5. Comparison of implantation results at 0 K and 300 K

In Fig. 4 the effect of the temperature on some of the properties of the implanted targets are shown for the

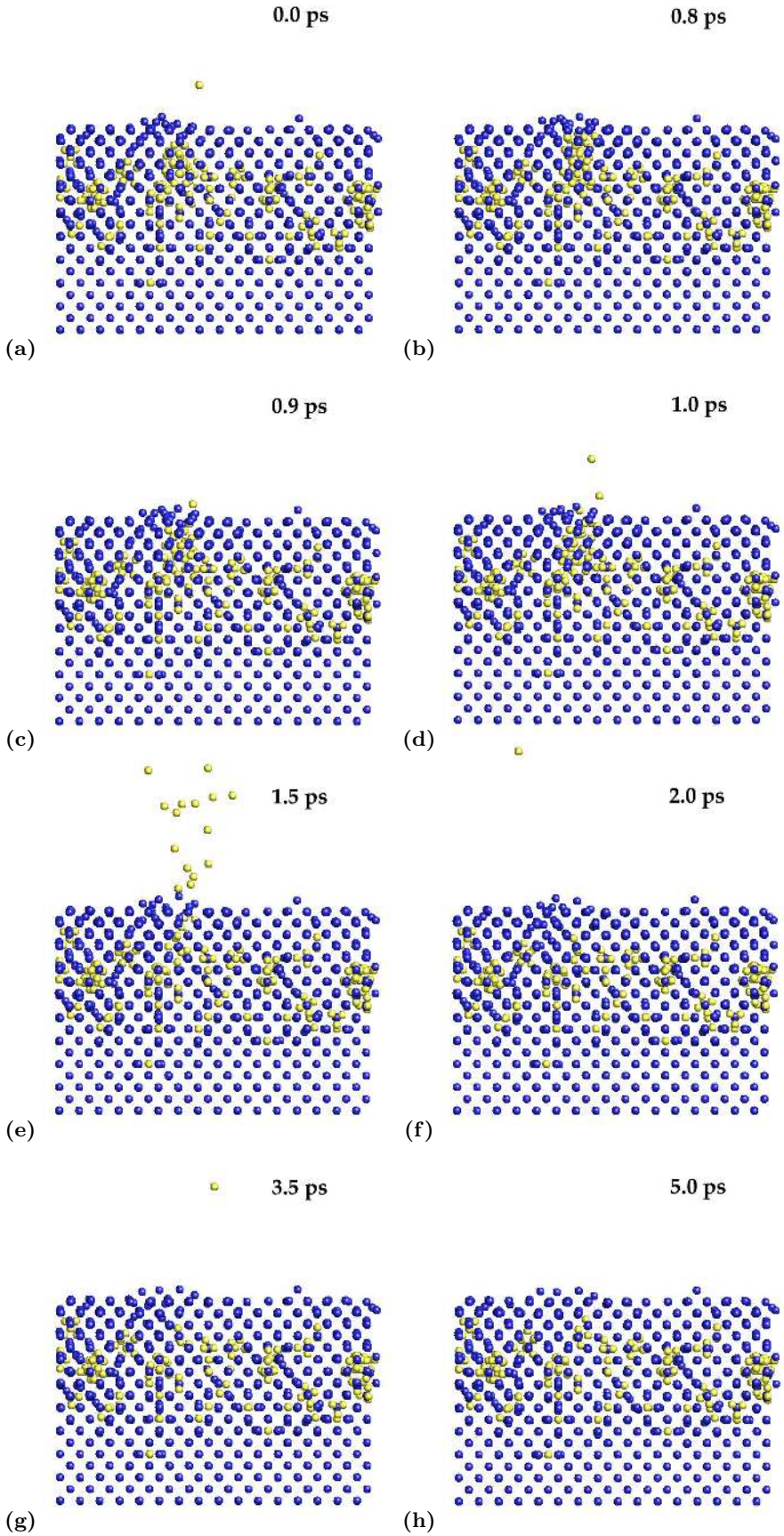

FIG. 3: Illustration of the cluster rupture in run 2027 in the 50 eV He series 1. (a) The 50 eV He ion is incident on the target. (b)-(c) He atoms in the surface-near cluster are escaping. (d) The cluster is being emptied. (e)-(g) Some He atoms are still leaving the former cluster. (h) Final relaxed state of the target.

50 eV He implantaion series 1. As expected, the retention and the number of clusters are smaller in the 300 K case, since the higher temperature makes the He atoms more mobile. This enables them to escape faster from the sample, and also to get trapped by other clusters more quickly.

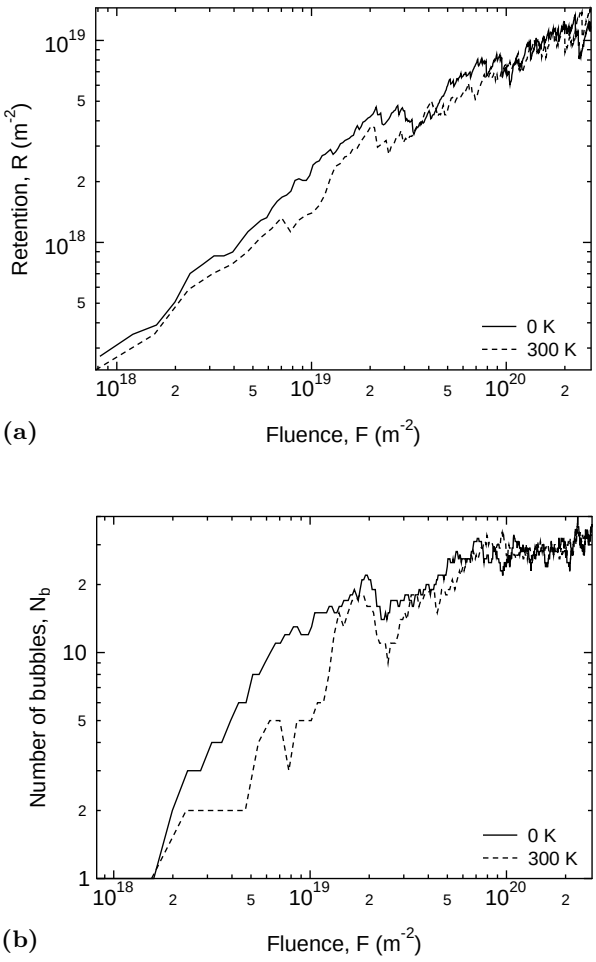

FIG. 4: (a) He retention and (b) the number of He clusters in the sample as a function of the He fluence, for the 50 eV implantation series with the sample at 0 K and 300 K, respectively.

6. *Summary of mechanisms*

By the results given above we may conclude that the clearest mechanisms for cluster growth are the formation of (111) crowdion interstitials or the punching out of interstitial loops.

We have illustrated the formation of crowdion interstitials in an earlier study[32]. An illustration of a loop-punching event is presented in Fig. 5.

D. Cluster properties as a function of fluence

In Fig. 6 the retention, the areal density of clusters, and the ratio of gas atoms to metal atoms in the implanted layer (down to the deepest lying He atom) are shown as a function of the fluence, for all the 50, 100, and 200 eV implantation series.

The erosion yield is shown in Table VIII. The largest yield value is of the order of 10^{-4}, except for the 200 eV He series. Disregarding this series, the erosion yield is somewhere between 0 and 5×10^{-4}. It should be noted that this erosion is in general not caused by the rupture of He clusters, it is more like physical sputtering. By this argument we will refer to this type of ejection of W atoms as sputtering, not erosion.

TABLE VIII: Yield of substrate erosion for the different implantation series. The yield is defined as N_e/N_i, where N_e is the number of eroded W atoms, and N_i is the number of implanted He ions.

Series	N_e	Yield of substrate erosion (N_e/N_i)
50 eV, series 1	0	0
50 eV, series 2	0	0
50 eV, series 1, $T = 300$ K	0	0
100 eV, series 1	0	0
100 eV, series 2	0	0
100 eV, series 3	2	$(3 \pm 2) \times 10^{-4}$
100 eV, series 4	1	$(1 \pm 1) \times 10^{-4}$
200 eV, series 1	4	$(8 \pm 4) \times 10^{-4}$

E. Cluster pressure

It might be of interest to know how the pressure required for *e.g.* loop punching to occur depends on the size of the cluster. In the literature there are several slightly different estimates (see Ref. 36 for a short review of these) for this critical pressure, denoted P_{LP}. Here we will use the relatively simple approximation[40]

$$P_{\mathrm{LP}} = \frac{2\gamma}{r} + \frac{\mu b}{r} \equiv \frac{C}{r}, \tag{1}$$

where $\gamma = 2.65$ N/m is the surface energy, $\mu = 158.6$ GPa the shear modulus, and b the Burger's vector of the loop. Putting $b \sim 1$ Å, one obtains $C = 21.16$ N/m $= 211.6$ GPa Å. Using the values in Table VI, and fitting the resulting (r, P) values to Eq. (1), we get $C = 23.646 \pm 0.006$ N/m, in good agreement with the theoretical estimate. The data and the fits are illustrated in Fig. 7.

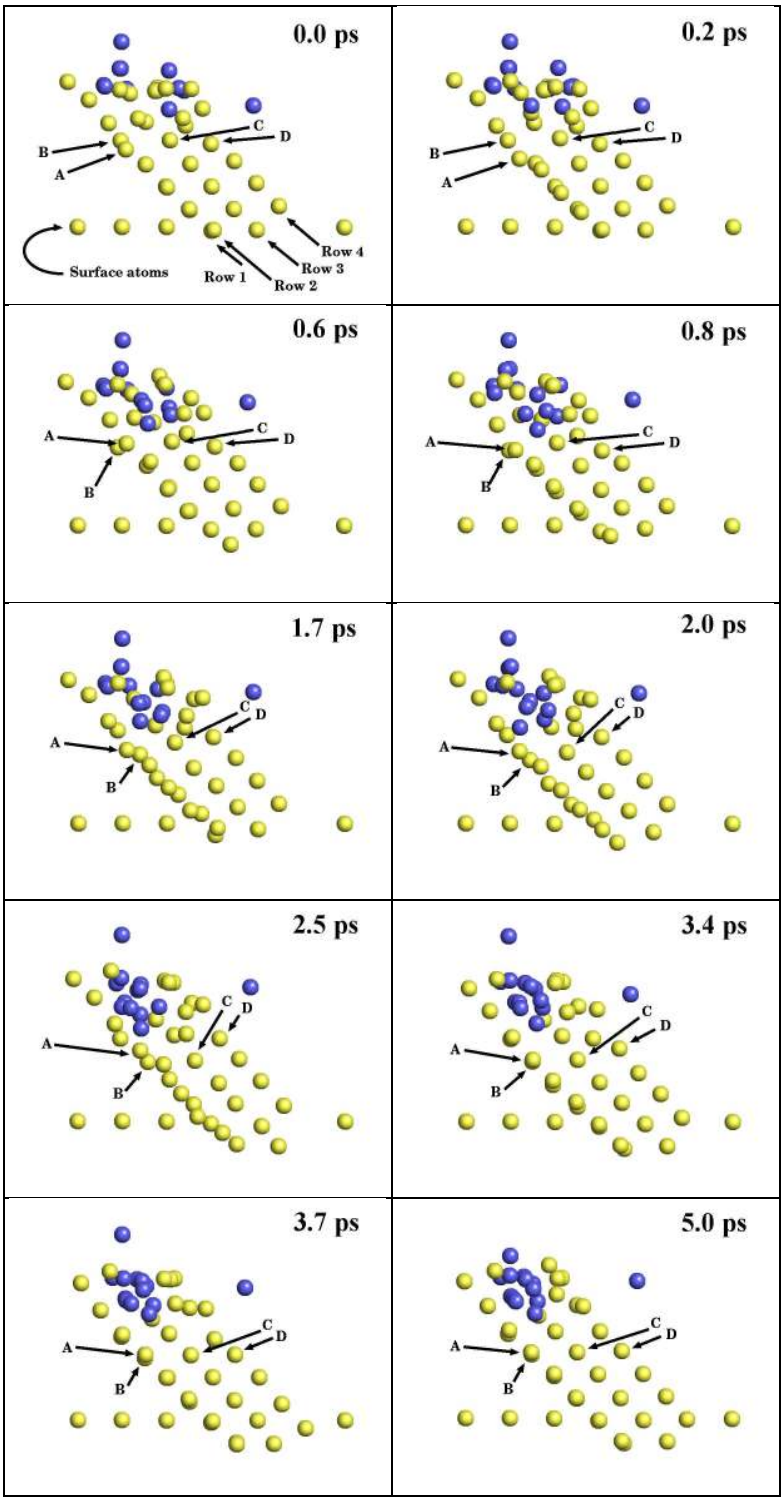

FIG. 5: Illustration of a loop punching event. **0.0 ps:** Initial configuration of atoms. Rows 1, 3 and 4 are clearly visible, row 2 is covered by row 1. Dark (blue) dots represent He atoms, light (yellow) dots represent W atoms. **0.2 ps:** Atoms in row 1 start to displace, especially atom A. **0.6 ps:** Atom A has relaxed backwards, atom B has moved slightly towards the surface. The surface atom in row 1 is close to making a displacement up onto the surface ... **0.8 ps:** ... but it is not able to go through with it. **1.7 ps:** The rows 1 and especially 2 are being compressed by the activity in the He cluster. Atoms in row 3 are about to start moving. Atoms in row 4 are off to a slow start. **2.0 ps:** Displacements in rows 1 and 2 are advancing. Atoms in row 3 are starting to move. **2.5 ps:** Atoms in rows 1 and 2 continue moving. The atoms in row 3 have been displaced by approximately one half the $\langle 111 \rangle$ distance. Atoms in row 4 have moved forward somewhat. **3.4 ps:** The atoms in rows 1 and 2 have relaxed backwards and have nearly completed their displacements. Atoms in row 3 are more or less in their final states, after having relaxed somewhat in the backward direction. Atoms in row 4 are in 'mid-flight'. **3.7 ps:** Atoms in row 4 are more or less in their final positions, but some relaxation of the surface-near atoms is still going on. **5.0 ps:** Final configuration of atoms. A total of 19 W atoms were directly involved in this loop punching event.

F. Cluster occupancies and superlattices

Runs from several 100 eV and 200 eV implantation series were investigated in order to obtain the distribution of cluster occupancy and to determine if any superlattices of He clusters had been formed. Run number 7000, corresponding to a fluence of 1.9×10^{27} He m^{-2} s^{-1} $\times 7000 \times$ 5 ps $= 6.65 \times 10^{19}$ He m^{-2} $\sim 10^{20}$ He m^{-2} was (arbitrarily) chosen. The cluster occupancy distributions are plotted in Fig. 8.

Pair correlation analysis was carried out on the clusters. In all cases the resulting distribution had only one peak near the origin, and decreased almost monotonically towards zero for larger distances, indicating that there were no cluster superlattice present.

IV. DISCUSSION

A. Probability of backscattering

From the results in Table I for the probability of backscattering, we find that there is a clear difference between the TRIMC and MDS results. TRIMC predicts a probability of about 0.52, which decreases slightly to 0.44 when the ion energy is increased from 20 eV to 1 keV. On the other hand, the MDS results indicate that the probability goes from 1.00 to 0.59 when the ion energy is increased from 20 eV to only 200 eV. However, the trend of decreasing probabilities towards the TRIM values is clear. The main difference between the TRIM and MD values is therefore mostly confined to the low energies, at which many-body atomic interactions become ingreasingly important. Since TRIM is designed for calculations of the range of energetic ions impinging on more or less stationary target atoms, it relies on the binary collision approximation to descibe atomic collisions. Therefore TRIM cannot be expected to give accurate results at low ion energies, compared to MD, which include many-body interactions.

B. Flux test

The results in Table II indicate that the average cluster depth remains at the same order of magnitude down to a flux of 8.660×10^{21} He m^{-2} s^{-1} $\sim 10^{22}$ He m^{-2} s^{-1}. This value coincides with the lower limit of the estimated He peak flux in ITER, which is 1% of the deuterium and tritium peak flux of 10^{24} ions m^{-2} s^{-1} (see sec. I B). In other words, this indicates that the results from the high-flux investigations carried out in this work should be relevant to studies using even the lower limit of the He flux in ITER.

C. Cluster nucleation and growth

The MDS results reveal that He atoms are able to cluster inside pure, single-crystalline W at initial sample temperatures of 0 and 300 K. This indicates that interstitial He atoms and clusters act as traps for other He atoms. The results also show that clusters can grow even under non-damaging irradiation. The clusters grow mainly by pushing out self-interstitial atoms (SIAs), preferentially in the (111) direction, thereby producing (111) crowdion interstitials and groups of these (interstitial dislocation loops).

As mentioned in the introduction (sec. I), it has been experimentally observed that a He cluster should contain at least about 10 He atoms before it is able to spontaneously push out a SIA when an additional He atom becomes trapped in it. In our MDS there seems to exist no such limit, even 'clusters' containing only two He atoms are able to create (111) crowdion interstitials when a third He atom becomes absorbed in it. This is due to the closeby surface, which offers much less opposition than a bulk region.

In our simulations the He clusters do not grow only by direct absorption of the incident He ions. Growth is possible also if the impinging He ion passes through the cluster on its way deeper into the target. Some of the kinetic energy of the He ion will be transferred to the cluster, which may become hot enough to punch out SIAs. Also, if the target has become 'porous' enough (containing a high concentration of small clusters) then the He clusters are able to communicate via interconnecting rows or lines of W atoms. If a cluster is unable to punch out SIAs directly, the increased pressure may be 'communicated' to a closeby cluster which is more able to create SIAs. In addition, He atoms becoming absorbed in a cluster may also come from clusters rupturing or leaking a small amount of He atoms.

The fact that clusters are formed, also at 300 K, is consistent with an estimate based on the diffusion constant. The largest linear displacement theoretically possible for the He atom after it has come to rest at the projected range is $d \equiv \sqrt{\langle R^2 \rangle} = \sqrt{6Dt}$, where D is the diffusion constant and t is the time the atom spends diffusing. We have previously (Ref. 32 and sec. II A) obtained $D_0 = (3.6 \pm 0.4) \times 10^{-8}$ m^2 s^{-1} and the migration energy $E_A = 0.29$ eV in the usual Arrhenius expression $D = D_0 e^{-E_M/(k_B T)}$. With $t = 5$ ps and $T = 300$ K one obtains $d = 0.038 \sim 10^{-2}$ Å. Clearly the time between implantations is not long enough to allow He atoms to escape through the surface, which results in a net deposition of He atoms inside the W sample.

In practice the migration rate may be somewhat higher, since the He atoms are relatively close to the surface and thus it is easier for them to somewhat push lattice atoms aside and move from one location to the next. Also, it should be pointed out that the He atoms 'migrate' (rather than collide with lattice atoms) in the lattice during the implantation, enabling them to trap at

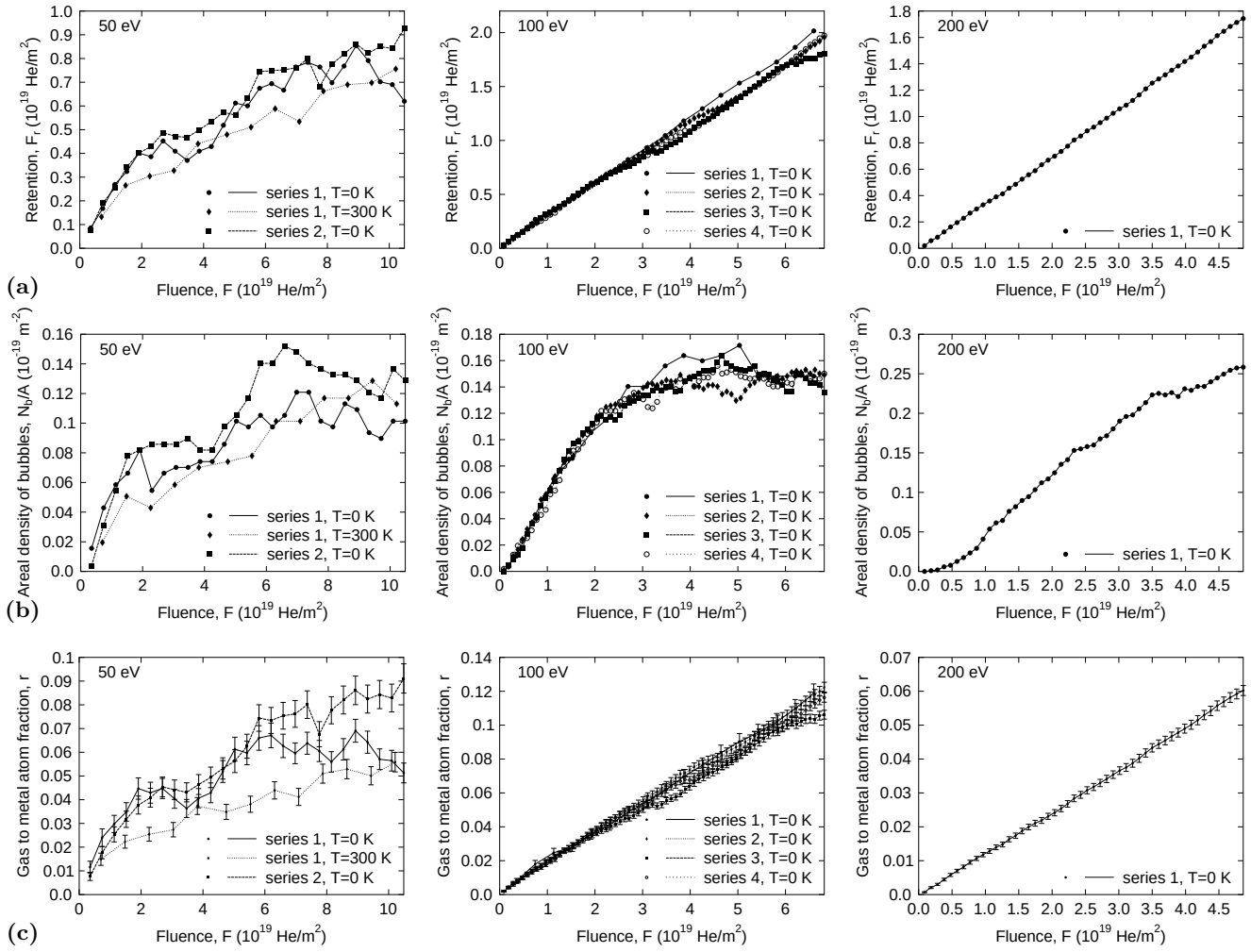

FIG. 6: (a) Retention, (b) areal density of clusters, and (c) the ratio of gas atoms to metal atoms in the implanted layer, as a function of fluence, for the 50, 100, and 200 eV He implantation series. The line curves are guides for the eye.

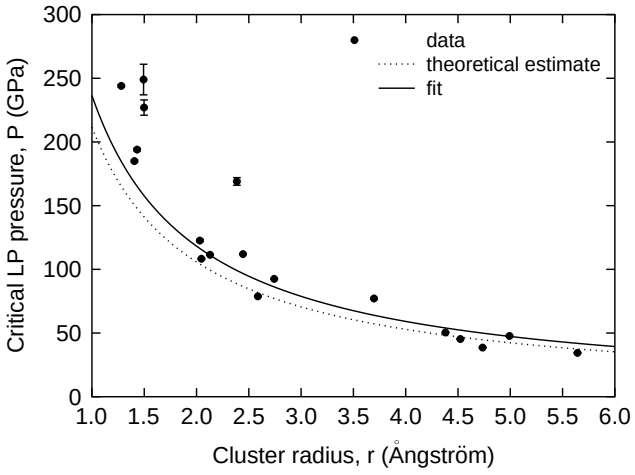

FIG. 7: Pressures in clusters before they undergo loop punching events, in the first series of 100 eV He implantation. The theoretical estimate of the critical pressure and and fit of the data to this expression are also shown.

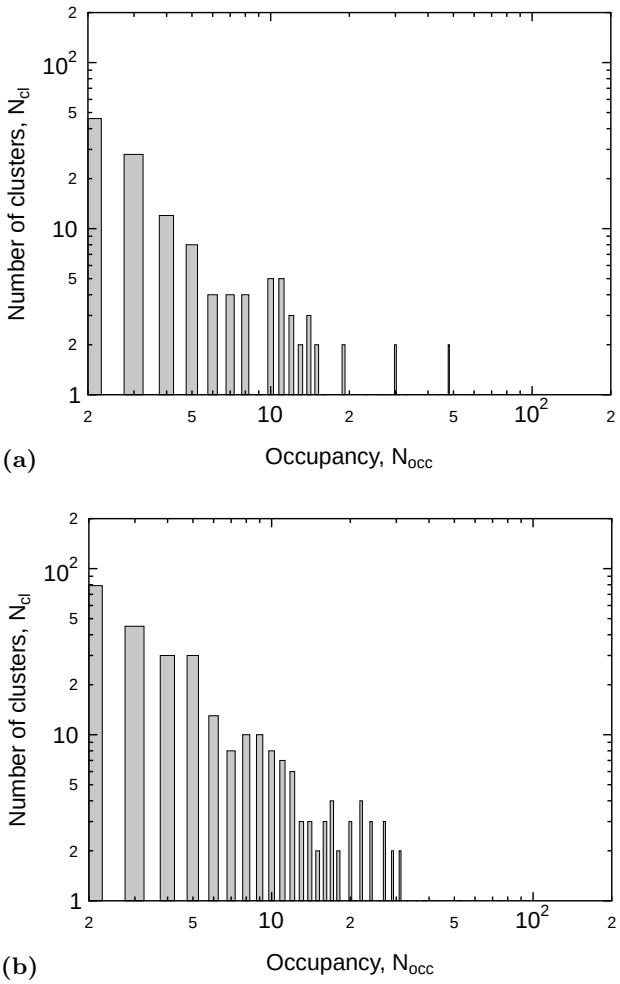

FIG. 8: Cluster occupancies at the end of run number 7000 for the 100 eV He series 1 (a) and 200 eV He series 1 (b).

clusters or escape from the lattice. In other words, the above result for the average displacement of implanted He atoms is to be considered only an estimate.

The present finding that non-damaging He irradiation is able to produce clusters in W also at room temperature (RT) is substantiated by experiments. In a field ion microscopy (FIM) study of 200 eV implantation of single-crystalline (011) W at RT carried out by Nicholson and Walls[41] it was observed that small 'voids' and dislocation loops were produced. However, Walls *et al.* [42] have pointed out that 'voids' observed by FIM are not necessarily real cavities — they can be regions of empty space, or they could be gas clusters. But since 200 eV He atoms have insufficient energy to create vacancies that may form the observed voids, and the temperature is relatively low for vacancies to be collected into voids from *e.g.* the surface, these 'voids' are most likely He clusters and not vacancy clusters.

He clusters have also been observed in poly-crystalline W samples irradiated with 250 eV at room temperature up to a fluence of 5.0×10^{20} He m^{-2} (Ref. 43). Platelets and dislocation loops of similar sizes were observed down to a depth of 200 Å already at a fluence of 0.14×10^{20} He m^{-2}.

D. Cluster properties as a function of fluence

From Fig. 6(a) it is clear that the retention increases when the ion energy becomes larger. The retention goes up with energy since the ions are penetrating deeper into the sample, and therefore are less able to get back to the surface and escape.

The (b) part of the figure shows that the number of clusters grows with increasing ion energy. This is reasomable, since higher energy means larger range and more energy deposition in the matrix, making cluster formation (but also ion escape through the surface) more likely. The fact that the 200 eV ions are going deeper affects the gas to metal atom ratio in the (c) part of the figure, which necessarily becomes smaller than for 50 eV and 100 eV ion implantation.

The results in Table VIII indicate that the substrate sputtering yield is between 0 and 5×10^{-4}. The experimental values[44] for the sputtering yield of polycrystalline W targets under He irradiation are about 4×10^{-4} (for 100 eV He ions) and 1×10^{-3} (for 200 eV He ions). Our yield values are in good agreement with these.

E. Cluster pressure

The theoretical pressure required for loop punching to occur is close to the pressures observed in our simulations. In fact, replotting Fig. 7 using a larger value than 1 Å for the Burger's vector b, it turns out that the theoretical critical pressure becomes larger than what is observed in our simulations. For example, using $b = 2.73$ Å (half the distance of the space diagonal in the BCC unit cell), we get that $P_{\rm LP}$ should be sligthly more than twice the value when using $b = 1$ Å. This is not in contradiction with our results, since the clusters are close to the surface and therefore need less pressure to punch out material.

Large He platelets (with an average radius of 200 Å (Ref. 36)) have been observed in Mo by Evans *et al.* [7] using 100-150 eV irradiation. The density in the platelets was calculated to be 2-3 He/V, and can be considered a good approximation of the true density[36], since the low-energy implantation is not likely to create small traps where He could reside undetected (and give rise to a smaller value for the density). The number density corresponds to the atomic density $\rho = (13-19)\times10^{22}$ He cm^{-3} $= 0.13 - 0.19$ He Å^{-3} (close-packing definition not used) and a pressure 9-35 GPa at 300 K according to the MLB expression.

These values may be compared to the last two simulated ones in Table VII. The atomic densities 0.286 He Å^{-3} and 0.301 He Å^{-3} of the relaxed clusters convert to 3.08 He/V and 3.25 He/V, respectively. The pressures are about 39 GPa and 34 GPa, and one may calculate cluster radii of 4.7 Å and 5.6 Å after approximating the clusters as spherical. Although our densities and pressures are larger than those estimated by Evans, the trend is clear from Table VII: the pressure and density in the cluster is reduced when the cluster size is increased. This is also seen from Fig. 7, where the simulated critical pressures for loop punching are shown. Therefore our simulated results are not in conflict with the experimental ones.

One may ask if these high pressures are reasonable, since they appear to be larger than the theoretical strength of the lattice. For Mo the strength can be estimated as $c_{44}/30 = 4$ GPa (Ref. 14), with $c_{44} = 120$ GPa (Ref. 36), making the MLB-EOS cluster pressure about 2-9 times the lattice strength. The theoretical strength of W is $c_{44}/30 = 160/30$ GPa ≈ 5 GPa, making the pressures in the above mentioned simulated clusters 7-8 times the lattice strength. Clearly the cluster pressures exceed the theoretical strength of the lattice in both these cases.

There are several possible reasons why the cluster pressures can be larger than the theoretically estimated strength of the crystal. First, the estimate is based on a simple analytical calculation[14]. Second, it assumes a geometry where the external force (or stress) causes planes of atoms to move relative to each other, whereas now the force on the lattice due to the high-pressure cluster is roughly spherically symmetric, the radius of curvature being quite small. Third, the pressure in the metal is significantly lower than that in the cluster just a few atomic layers from the interface. This is possible, since the boundary conditions for the stress tensor do not require that each tensor element (*e.g.* the hydrostatic pressures) be continous across the border[45].

F. Cluster occupancies and superlattices

The absence of cluster superlattices is no surprise, since the high flux value in combination with the quench at the end of each individual implantation limits the time each incident He atom can spend freely migrating in the lattice. This leads to a limited mobility of He atoms, ruling out any homogenization in size of the clusters. The finding of cluster superlattices by Johnson and Mazey[46] in W and other BCC metals does not contradict our results, since in they used 50 keV He ions and an implantation temperature of 773 K. These conditions should be enough to create vacancies and keep them and the He ions mobile, enabling a more homogenous growth of clusters.

V. CONCLUSIONS

It was found that non-damaging He irradiation of tungsten (helium ion energy less than about 500 eV) at 0 and 300 K can produce He clusters containing up to the order of 100 atoms. The athermal nucleation of the clusters proceeds via the creation of (111) crowdion interstitials and groups of these, *i.e.* interstitial dislocation loops. No strict limit was found for the minimum occupancy of a cluster required to be able to produce self-interstitial atoms was found. This is mainly attributable to the closeby surface, which offers less opposition than the bulk. Insignificant erosion of tungsten atoms was observed, but not in conjunction with rupturing clusters.

Acknowledgments

The research was supported by the Academy of Finland under project No. 48751 and by the University of Helsinki under the NAPROMA project.

* Electronic address: krister.henriksson@helsinki.fi

[1] B. M. U. Scherzer, *Development of surface topography due to gas ion implantation* (Springer, Berlin, Germany, 1983), vol. II of *Sputtering by Particle Bombardment*, chap. 7, pp.

271–355.
[2] R. S. Barnes, G. B. Redding, and A. H. Cottrell, Phil. Mag. **3**, 97 (1958).
[3] S. L. Sass and B. L. Eyre, Phil. Mag. **27**, 1447 (1973).
[4] D. J. Mazey, B. L. Eyre, J. Evans, S. K. Erents, and G. M. McCracken, J. Nucl. Mater. **64**, 145 (1977).
[5] L. M. Caspers, R. H. J. Fastenau, A. van Veen, and W. F. W. M. van Heugten, Phys. Stat. Sol. (a) **46**, 541 (1978).
[6] M. S. A. E. Keriem, D. P. van der Werf, and F. Pleiter, Hyperfine Interactions **79**, 787 (1993).
[7] J. H. Evans, A. van Veen, and L. M. Caspers, Nature **291**, 310 (1981).
[8] E. V. Kornelsen, Radiat. Eff. **13**, 227 (1972).
[9] E. V. Kornelsen and A. A. van Gorkum, J. Nucl. Mater. **92**, 79 (1980).
[10] G. J. van der Kolk, A. van Veen, L. M. Caspers, and J. T. M. de Hosson, J. Nucl. Mat. **127**, 56 (1985).
[11] G. J. Thomas, W. A. Swansiger, and M. I. Baskes, J. Appl. Phys. **50**, 6942 (1979).
[12] W. D. Wilson, C. L. Bisson, and M. I. Baskes, Phys. Rev. B **24**, 5616 (1981).
[13] G. J. Thomas and R. Bastasz, J. Appl. Phys. **52**, 6426 (1981).
[14] C. Kittel, *Introduction to solid state physics* (Wiley, 1996), 7th ed.
[15] V. Barabash, G. Federici, R. Matera, A. R. Raffray, and I. H. Teams, Phys. Scripta **T81**, 74 (1999).
[16] G. Federici and et al., J. Nucl. Mater. **266-269**, 14 (1999).
[17] G. Federici, H. Wuerz, G. Janeschitz, and R. Tivey, Fusion Eng. and Design **61-62**, 81 (2002).
[18] R. A. Causey and T. J. Venhaus, Phys. Scripta **T94**, 9 (2001).
[19] F. C. Sze, R. P. Doerner, and S. Luckhardt, J. Nucl. Mat. **264**, 89 (1999).
[20] A. A. Haasz, M. Poon, and J. W. Davis, J. Nucl. Mat. **266-269**, 520 (1999).
[21] W. Wang, J. Roth, S. Lindig, and C. H. Wu, J. Nucl. Mat. **299**, 124 (2001).
[22] K. O. E. Henriksson, K. Nordlund, and J. Keinonen, *Difference in formation of hydrogen and helium clusters in tungsten*, submitted to *Appl. Phys. Letters*.
[23] K. Nordlund, M. Ghaly, R. S. Averback, M. Caturla, T. D. de la Rubia, and J. Tarus, Phys. Rev. B **57**, 7556 (1998).
[24] H. J. C. Berendsen, J. P. M. Postma, W. F. van Gunsteren, A. D. Nola, and J. R. Haak, J. Chem. Phys. **81**, 3684 (1984).
[25] W. D. Wilson and C. L. Bisson, Radiat. Eff. **19**, 53 (1973).
[26] A. Wagner and D. N. Seidman, Phys. Rev. Lett. **42**, 515 (1979).
[27] J. Amano and D. N. Seidman, J. Appl. Phys. **56**, 983 (1984).
[28] D. R. Lide, *CRC Handbook of Chemistry and Physics* (CRC Press LLC, Boca Raton, FL, USA, 2001), 82nd ed.
[29] F. Maury, M. Biget, P. Vajda, A. Lucasson, and P. Lucasson, Radiat. Eff. **38**, 53 (1978).
[30] G. J. Ackland and R. Thetford, Phil. Mag. A **56**, 15 (1987).
[31] DMol is a trademark of AccelRys. Inc.
[32] K. O. E. Henriksson, K. Nordlund, J. Keinonen, D. Sundholm, and M. Patzschke, Physica Scripta **T108**, 95 (2004).
[33] H. Trinkaus and W. G. Wolfer, J. Nucl. Mater. **122-123**, 552 (1984).
[34] J. B. Condon and T. Schober, J. Nucl. Mater. **207**, 1 (1993).
[35] R. L. Mills, D. H. Liebenberg, and J. C. Bronson, Phys. Rev. B **21**, 5137 (1980).
[36] S. E. Donnelly, Radiat. Eff. **90**, 1 (1985).
[37] J. F. Ziegler, SRIM-2003 software package, available online at *http://www.srim.org*.
[38] K. A. Fichthorn and W. H. Weinberg, J. Chem. Phys. **95**, 1090 (1991).
[39] A. B. Bortz, M. H. Kalos, and J. L. Lebowitz, J. Computational Physics **17**, 10 (1975).
[40] H. Trinkaus, Radiat. Eff. **78**, 189 (1983).
[41] R. J. K. Nicholson and J. M. Walls, J. Nucl. Mater. **76-77**, 251 (1978).
[42] J. M. Walls, R. M. Boothby, and H. N. Southworth, Surface Science **61**, 419 (1976).
[43] H. Iwakiri, K. Yasunaga, K. Morishita, and N. Yoshida, J. Nucl. Mat. **283-287**, 1134 (2000).
[44] H. H. Andersen and H. L. Bay, in *Sputtering by Particle Bombardment I*, edited by R. Behrisch (Springer, Berlin, Germany, 1981), vol. 47 of *Topics in Applied Physics*, chap. 4, pp. 145–218.
[45] A. L. Fetter and J. D. Walecka, *Theoretical mechanics of particles and continua* (McGraw-Hill, 1980).
[46] P. B. Johnson and D. J. Mazey, J. Nucl. Mater. **218**, 273 (1995).
[47] We will frequently use 'ion' instead of 'atom' for any particle incident on a sample, although our MDS do not discriminate between charged and neutral atoms.